Journal of Sound and Vibration (2002) **251**(5), 891–903
doi:10.1006/jsvi.2001.4019, available online at http://www.idealibrary.com on IDEAL®

IMPLEMENTATION OF A BROADBAND DUCT ANC SYSTEM USING ADAPTIVE SPATIALLY FEEDFORWARD STRUCTURE

M. R. Bai and P. Zeung

Department of Mechanical Engineering, National Chiao-Tung University, 1001 *Ta-Hsueh Road, Hsin-Chu* 30010, *Taiwan, Republic of China. E-mail*: *msbai@cc.nctu.edu.tw*

(*Received* 26 *April* 2000, *and in final form* 10 *August* 2001)

An adaptive spatially feedforward algorithm is proposed for broadband attenuation of noise in ducts. Acoustic feedback generally exists in this active noise control structure. Munjal and Eriksson (1988 *Journal of Acoustical Society of America* **84**, 1086–1093) derived an ideal controller for the spatially feedforward structure. The ideal controller can be partitioned into two parts. The first part represents a *repetitive controller* that can be implemented by an infinite impulse response (IIR) filter, whereas the second part represents the dynamics of transducer that can be implemented by a finite impulse response (FIR) filter. In the paper, the IIR filter is merged with the original plant. The FIR filter is adaptively updated by the least-mean-square (LMS) algorithm to accommodate perturbations and uncertainties in the system. The proposed algorithm is implemented via a floating point digital signal processor and compared with other commonly used algorithms such as the Filtered-X LMS algorithm, the feedback neutralization algorithm, and the Filtered-U LMS algorithm. Experimental results show that the system has attained 15·7 dB maximal attenuation in the frequency band 200–600 Hz.

1. INTRODUCTION

Active noise control (ANC) [1–3] techniques provide numerous advantages over conventional passive methods such as improved low-frequency performance, reduction of physical size and weight, zero back pressure programmable flexibility, and so forth. In ANC applications to date, feedforward control has been widely used whenever a non-acoustical reference is available [4]. In practice, however, a non-acoustical reference required by feedforward control is usually unavailable. The spatially feedforward control structure (Figure 1(a)) appears to be a more feasible approach in dealing with such situations, especially when broadband attenuation is sought [5–7]. In the spatially feedforward control structure, an upstream sensor is placed near the primary source. The upstream sensor captures not only the primary noise but also the signals from the downstream control source. The control structure is thus not actually feedforward but only "spatially" feedforward.

An in-depth analysis of the spatially feedforward structure was conducted by Munjal and Eriksson [8]. Their investigation reveals that there exists an ideal controller for such an ANC structure. The ideal controller can be partitioned into two parts. The first part represents a repetitive controller that can be implemented by an infinite impulse response (IIR) filter, whereas the second part represents the dynamics of transducer that can be implemented by a finite impulse response (FIR) filter. In our method, a fixed IIR filter is

0022-460X/02/$35.00

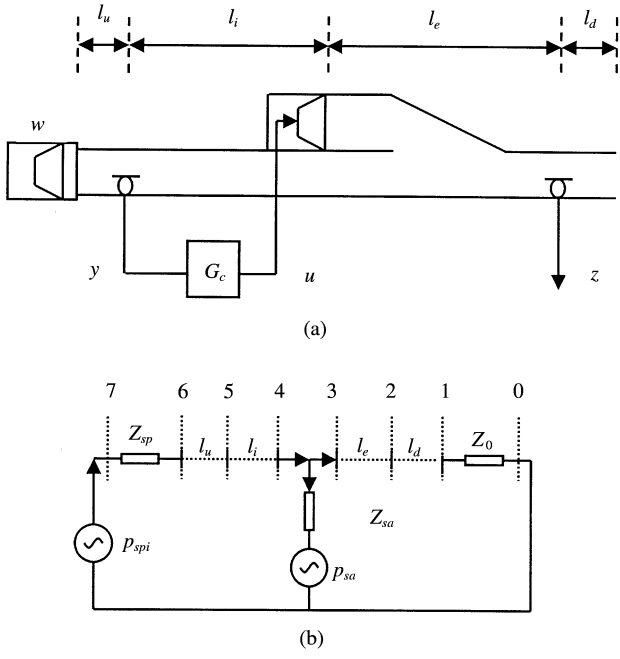

Figure 1. The spatially feedforward structure. (a) The ANC system of a duct; and (b) the equivalent circuit.

merged with the original plant. In addition, an FIR filter (generally of low order) is adaptively updated by the least-mean-square (LMS) algorithm to accommodate perturbations as well as uncertainties in the system. The proposed algorithm is implemented on the platform of a floating point digital signal processor (DSP) and compared with other commonly used algorithms such as the Filtered-X LMS (FXLMS) algorithm, the feedback neutralization algorithm, and the Filtered-U LMS (FULMS) algorithm. Experiments are carried out to validate the proposed ANC approach for attenuation of the random noise in a long duct. Experimental results show that the system attained 15·7 dB maximal attenuation within the frequency band 200–600 Hz.

2. SPATIALLY FEEDFORWARD CONTROLLER FOR DUCT

The spatially feedforward structure of a duct and its equivalent circuit are shown in Figure 1. Munjal and Eriksson [8] derived an ideal controller for achieving global noise cancellation downstream the control source in a finite-length duct:

$$C_{ideal} = -\frac{Z_{sa}}{Y_0}\left(\frac{\mathrm{e}^{-\mathrm{j}kl_i}}{1-\mathrm{e}^{-2\mathrm{j}kl_i}}\right) \tag{1}$$

$$= C_0 C_r,$$

where Z_{sa} is the acoustic impedance of the control source, $Y_0 = c/S$ is the characteristic impedance of the duct, c is the sound speed, S is the cross-sectional area of the duct, k is the wave number, and l_i is the distance between the upstream measurement microphone and the control source. In equation (1), $C_0 \equiv -Z_{sa}/Y_0$ is a function of the finite impedance Z_{sa}

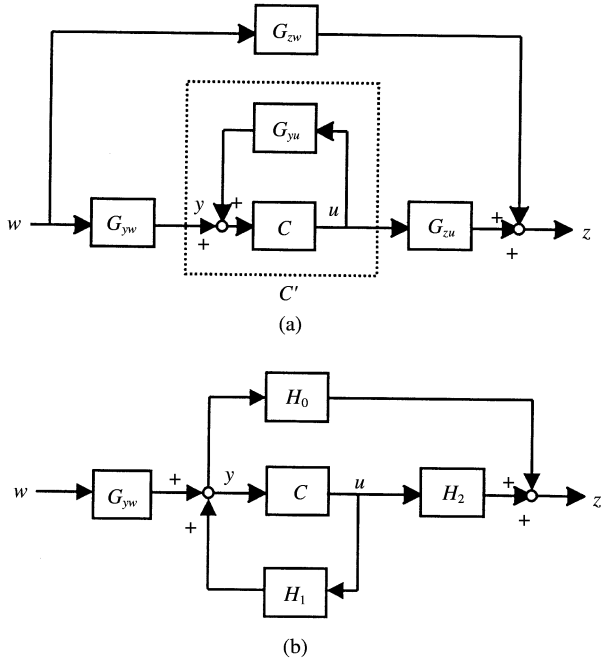

Figure 2. Two equivalent spatially feedforward controllers. (a) Block diagram of zero spillover controller and (b) block diagram of the Roure's controller.

which depends only on the electro-mechanical constants of the control source. On the other hand, $C_r \equiv e^{-2jkl_i}/(1 - e^{-2jkl_i})$ takes the form of the so-called *repetitive controller* [9].

The zero spillover controller [7] is shown in Figure 2(a), where w, y, z and u are exogenous noise, measurement, performance variable and control input, respectively; the transfer functions G's are self-explanatory from the subscripts:

$$C_{ZSP}(j\omega) = \frac{G_{zw}(j\omega)}{G_{zw}(j\omega)G_{yu}(j\omega) - G_{zu}(j\omega)G_{yw}(j\omega)}. \tag{2}$$

This controller requires the knowledge of the disturbance-related transfer functions G_{zw} and G_{yw} that are generally unavailable in practice. To resolve the problem, a more practical but equivalent controller proposed by Roure [10] can be used. It is obtained by dividing the numerator and the denominator of equation (2) by $G_{yw}(j\omega)$:

$$G_{ZSP}(j\omega) = \frac{-G_{zw}(j\omega)/G_{yw}(j\omega)}{G_{zw}(j\omega) - G_{yu}(j\omega)\, G_{zw}(j\omega)/G_{yw}(j\omega)}$$

$$= \frac{-H_0(j\omega)}{H_2(j\omega) - H_1(j\omega)H_0(j\omega)} \equiv C_{Roure}(j\omega), \tag{3}$$

where $H_0(j\omega) \equiv G_{zw}(j\omega)/G_{yw}(j\omega)$ is the frequency response function between the pressures measured at the performance microphone and the measurement microphone (Figure 3), $H_1(j\omega) \equiv G_{yu}(j\omega)$ is the frequency response function between the measurement microphone and the control speaker, and $H_2(j\omega) \equiv G_{zu}(j\omega)$ is the frequency response function between the performance microphone and the control speaker. It is noted that all functions of

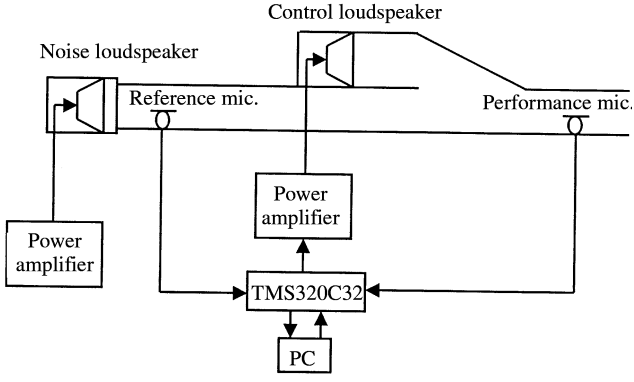

Figure 3. The experimental set-up of a spatially feedforward ANC system.

equation (3) are measurable. The block diagram of the Roure's controller is shown in Figure 2(b).

Next, we will prove the equivalence between the zero spillover controller and the ideal controller. Using Munjal and Eriksson's [8] notations, the transfer functions, G_{yw}, G_{zw}, G_{yu}, and G_{zu} can be identified as $G_{yw} = p_{5p}/p_{spi}$, $G_{zw} = p_{3p}/p_{spi}$, $G_{yu} = p_{5a}/p_{sa}$, and $G_{zu} = p_{3a}/p_{sa}$, where p_{spi} is the acoustic pressure of the primary source, p_{sa} is the acoustic pressure of the auxiliary source, p_{3a} is the acoustic pressure of location 3 in Figure 1(b) with only the auxiliary source on, and p_{3p} is the acoustic pressure of location 3 in Figure 1(b) with only the primary source on, etc. One can then manipulate the zero spillover controller of equation (2) as follows:

$$C_{ZSP}(\mathrm{j}\omega) = \frac{G_{zw}(\mathrm{j}\omega)}{G_{zw}(\mathrm{j}\omega)G_{yu}(\mathrm{j}\omega) - G_{zu}(\mathrm{j}\omega)G_{yw}(\mathrm{j}\omega)}$$

$$= \frac{[p_{3p}/p_{spi}]}{[p_{3p}/p_{spi}][p_{5a}/p_{sa}] - [p_{3a}/p_{sa}][p_{5p}/p_{spi}]}$$

$$= \frac{[\zeta_e/Z_{spi}VR]}{[\zeta_e/Z_{spi}VR][\zeta_e/Z_{sa}VR] - [\zeta_e/Z_{sa}(C_i + \mathrm{j}Y_0S_i/Z_{spi})/VR][\zeta_eC_i + \mathrm{j}Y_0S_i + \mathrm{j}Y_0S_i\zeta_e/Z_{sa}/Z_{spi}VR]}$$

$$= \frac{Z_{sa}VR}{\zeta_e - (C_i + \mathrm{j}Y_0S_i/Z_{spi})(\zeta_eC_i + \mathrm{j}Y_0S_i + \mathrm{j}Y_0S_i\zeta_e/Z_{sa})}$$

$$\sim \frac{Z_{sa}VR}{-\mathrm{j}Y_0S_iVR}$$

$$= \frac{\mathrm{j}Z_{sa}}{Y_0S_i} = -\frac{Z_{sa}}{Y_0}\left(\frac{\mathrm{e}^{-\mathrm{j}k_0l_i}}{1 - \mathrm{e}^{-2\mathrm{j}k_0l_i}}\right) = C_{ideal}(\mathrm{j}\omega). \tag{4}$$

Therefore in this paper, we chose the equivalent but simpler approach proposed by Roure [11] to implement the ideal controller for the following three reasons. First, as indicated by equation (4), the ideal controller is essentially of infinite bandwidth and may produce excessive control output at high frequency. The excessive output beyond the control

bandwidth is likely to saturate, and even destabilize the system. Second, errors exist in the identified electro-mechanical–acoustical parameters of the system. Third, there is always some dynamics of the physical system that cannot be modelled by the simple lumped-parameter model.

3. ADAPTIVE SPATIALLY FEEDFORWARD ANC ALGORITHM

3.1. REVIEW OF SOME LMS-BASED ALGORITHMS

In what follows, a brief review of some widely used LMS-based algorithms including the FXLMS algorithm, the feedback neutralization algorithm, and the FULMS algorithm will be given [12]. The block diagram of ANC system using the FXLMS algorithm is shown in Figure 4(a). The error signal is expressed as

$$e(n) = d(n) - y'(n) = d(n) - s(n) * y(n) = d(n) - s(n) * [w^{\mathrm{T}}(n)\bar{x}(n)], \tag{5}$$

where $s(n)$ is the impulse response of secondary path $S(z)$ at the time n, $*$ denotes the linear convolution, $w(n) = [w_0(n) w_1(n) \dots w_{L-1}(n)]^{\mathrm{T}}$ is the coefficient vector of the FIR filter $W(z)$, $\bar{x}(n) = [x(n) x(n-1) \dots x(n-L+1)]^{\mathrm{T}}$ is the reference signal vector, and L is the order of filter $W(z)$. The FXLMS method minimizes the instantaneous squared error $\hat{\xi}(n) = e^2(n)$ and updates the coefficient vector in the negative gradient direction with step size μ:

$$w(n+1) = w(n) - \frac{\mu}{2} \nabla \hat{\xi}(n) = w(n) + \mu \bar{x}'(n) e(n). \tag{6}$$

It should be noted that the effect of acoustic feedback is not considered in the FXLMS algorithm using feedforward structure.

The second approach that deals with the undesirable acoustic feedback problem is to use a feedback neutralization filter within the controller. An ANC system using the FXLMS algorithm with feedback neutralization is illustrated in Figure 4(b). The feedback signal to the reference microphone is cancelled "electronically" by using a feedback neutralization filter $\hat{F}(z)$ which models the transfer function from the loudspeaker input to the reference microphone output. Thus, the input signal $x(n)$ is computed as

$$x(n) = u(n) - \sum_{m=0}^{M-1} \hat{f}_m y(n-m-1), \tag{7}$$

where $u(n)$ is the signal from the reference microphone, $\hat{f}_m$ are the coefficients of the Mth order feedback neutralization filter $\hat{F}(z)$, and $y(n)$ is the cancelling signal. With the removal of acoustic feedback, the optimal controller can be found by ordinary FXLMS algorithm.

Finally, ANC system using the FULMS algorithm is illustrated in Figure 4(c). Similar to the FXLMS filter, the steepest-descent algorithm is used to search for the optimal controller which in FULMS is an IIR filter. However, the search process could possibly be trapped in local minima because the cost function in this case is not a quadratic function. The update formula of the filter coefficients in the FULMS algorithm is

$$w(n+1) = w(n) + \mu [\hat{s}(n) * u(n)] e(n) = w(n) + \mu u'(n) e(n), \tag{8}$$

where μ is the step size, $\hat{s}$ is the estimated secondary path, $e(n)$ is the error signal, $u'(n) = \hat{s}(n) * u(n)$,

$$u(n) = \begin{bmatrix} x(n) \\ y(n-1) \end{bmatrix}$$

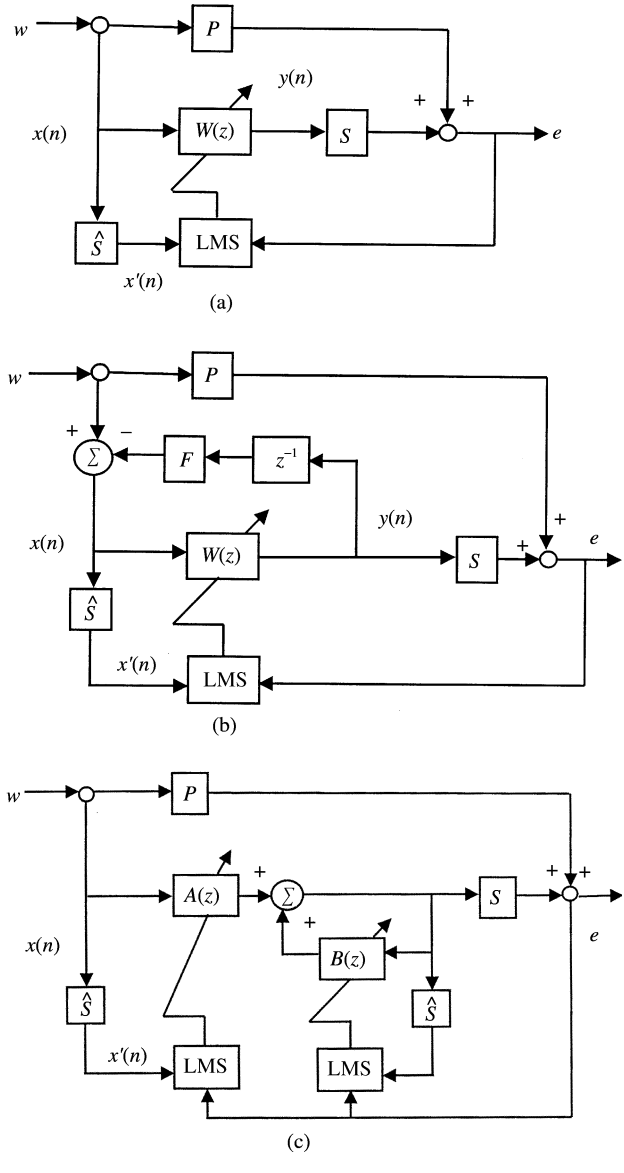

Figure 4. Some commonly used LMS-based ANC algorithms. (a) Block diagram of the FXLMS algorithm; (b) block diagram of the feedback neutralization algorithm; and (c) block diagram of the FULMS algorithm.

is a generalized reference vector, and

$$w(n) = \begin{bmatrix} a(n) \\ b(n) \end{bmatrix}$$

is an overall weight vector. Equation (8) can be further partitioned into two vector equations for adaptive filters $A(z)$ and $B(z)$ representing the numerator term and the denominator term, respectively, of the IIR filter in the FULMS algorithm.

$$a(n+1) = a(n) + \mu x'(n)e(n) \quad \text{and} \quad b(n+1) = b(n) + \mu \hat{y}'(n-1)e(n), \tag{9}$$

where $x'(n) = \hat{s}(n) * x(n)$ and $\hat{y}'(n-1) = \hat{s}(n) * y(n-1)$.

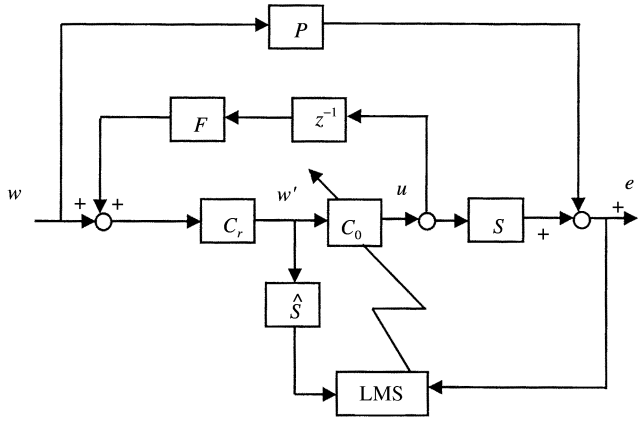

Figure 5. Block diagram of the adaptive spatially feedforward algorithm.

3.2. ADAPTIVE SPATIALLY FEEDFORWARD ALGORITHM

In this section, an adaptive spatially feedforward algorithm will be developed for the spatially feedforward structure. The aforementioned Munjal's ideal controller is repeated here for convenience,

$$C_{ideal} = -\frac{Z_{sa}}{Y_0}\left(\frac{e^{-jkl_i}}{1-e^{-2jkl_i}}\right). \tag{10}$$

In viewing equation (10), we make a proposition that the ANC controller should take the form

$$C = C_0 C_r, \tag{11}$$

where C_0 approximates the transducer dynamics (generally of low order FIR form) and C_r approximates the repetitive controller (generally of IIR form), i.e., $C_r \approx e^{-jkl_i}/(1-e^{-jk2l_i})$. The repetitive patterns in the frequency response and the impulse response of the controller shall be seen in the experimental results. The repetitive peaks with nearly equal interval in the time domain and in the frequency domain are actually created by acoustic feedback in the spatially feedfordward structure.

From the discussion in section 2, we are able to decompose Roure's controller into C_0 and C_r because of its equivalence to Munjal's ideal controller. The idea of the adaptive spatially feedforward algorithm is shown in Figure 5. In the case where the temperature of the duct is not varied much, the repetitive peaks of the ideal controller are almost fixed. Thus, the transfer function, C_r, is implemented by a fixed IIR filter fitting the repetitive peaks in the frequency response of Roure's controller. On the other hand, in order to accommodate system uncertainties and perturbations which frequently occur in practice, the transfer function, C_0, is realized by an FIR filter adaptively updated by a modified FXLMS algorithm.

$$u = C_0 * w', \qquad w' = C_r * w, \tag{12, 13}$$

$$C_0(k+1) = C_0(k) - \mu \frac{2eS}{(1-C_r C_0 F)^2} w'. \tag{14}$$

Note, however, that the filter function $S/(1 - C_r C_0 F)^2$ in the update formula of equation (14) contains a term C_0 which prevents direct implementation of the update algorithm. To alleviate the difficulty, the feedback term in equation (14) is neglected to get a simplified and workable update law for the filter weights

$$C_0(k+1) = C_0(k) - \mu e(k) * (S * w'), \tag{15}$$

where C_0 and S are realized by FIR filters, and "$*$" denotes linear convolution. Although the instant gradient estimate in the update law is somewhat biased, the latter experimental verification shows that such a heuristic approach is effective for the spatially feedfordward structure.

4. EXPERIMENTAL INVESTIGATION

4.1. EXPERIMENTAL RESULTS

A duct made of plywood shown in Figure 3 is used for verifying the proposed ANC method. The length of the duct is 440 cm and the cross-section is 25 cm × 25 cm. There is 10 cm between the primary source speaker and the measurement microphone. To reduce acoustic feedback, we use the backward control loudspeaker facing the open end of the duct. The distance between the measurement microphone and the control speaker is 235 cm to ensure causality of the controller. The distance between the control speaker and the performance microphone is 110 cm. A TMS320C32 DSP equipped with four 16-bit analog IO channels is utilized to implement different controllers. The sampling frequency is chosen to be 2 kHz. Considering the cut-off frequency of the duct ($\sim$ 700 Hz) and the poor response of speaker at low frequency, we chose control bandwidth from 200 to 600 Hz.

In the following experiments, the FXLMS algorithm, the feedback neutralization algorithm, and the FULMS algorithm are compared for the spatially feedfordward structure. The FXLMS is first examined by using the reference signal from the upstream measurement microphone. As expected, this algorithm failed to attain noise attenuation (Figure 6(a)).

Next, we implement the feedback neutralization method that subtracts the signals from the feedback path to produce a non-contaminated reference input. What should be noted is that there is an inherent one sample delay in the feedback between $F(z)$ and $\hat{F}(z)$ because when the reference sample $u(n)$ is measured, the output $y(n)$ has not yet been computed. The experimental result of control performance obtained from this method is shown in Figure 6(b).

As a third approach, the FULMS algorithm is implemented by using identical filter order and step size to update the feedforward $B(z)$ and the feedback filters $A(z)$. The experimental result of control performance is shown in Figure 6(c).

In addition to the commonly used methods mentioned previously, an experiment was conducted for verifying the adaptive spatially feedfordward ANC algorithm proposed in this paper. First, we calculate the frequency response of Roure's controller, as shown in Figure 7(a) via measurement of three frequency responses, i.e., H_0, H_1, and H_2 in Figure 2(b). While measuring frequency responses H_1 and H_2, the primary speaker is switched off and the control speaker is switched on. Then, the control speaker is switched off and the primary speaker is switched on to measure H_0. Second, we curve-fit the repetitive peaks of the frequency response of Roure's controller in the control bandwidth to obtain an IIR filter representation of C_r in equation (11). The frequency response regenerated by the identified model and the original frequency response of the controller are compared in Figure 7(a). MATLAB functions, *invfreqz tf2sos* are employed in this proceudre [13]. The function

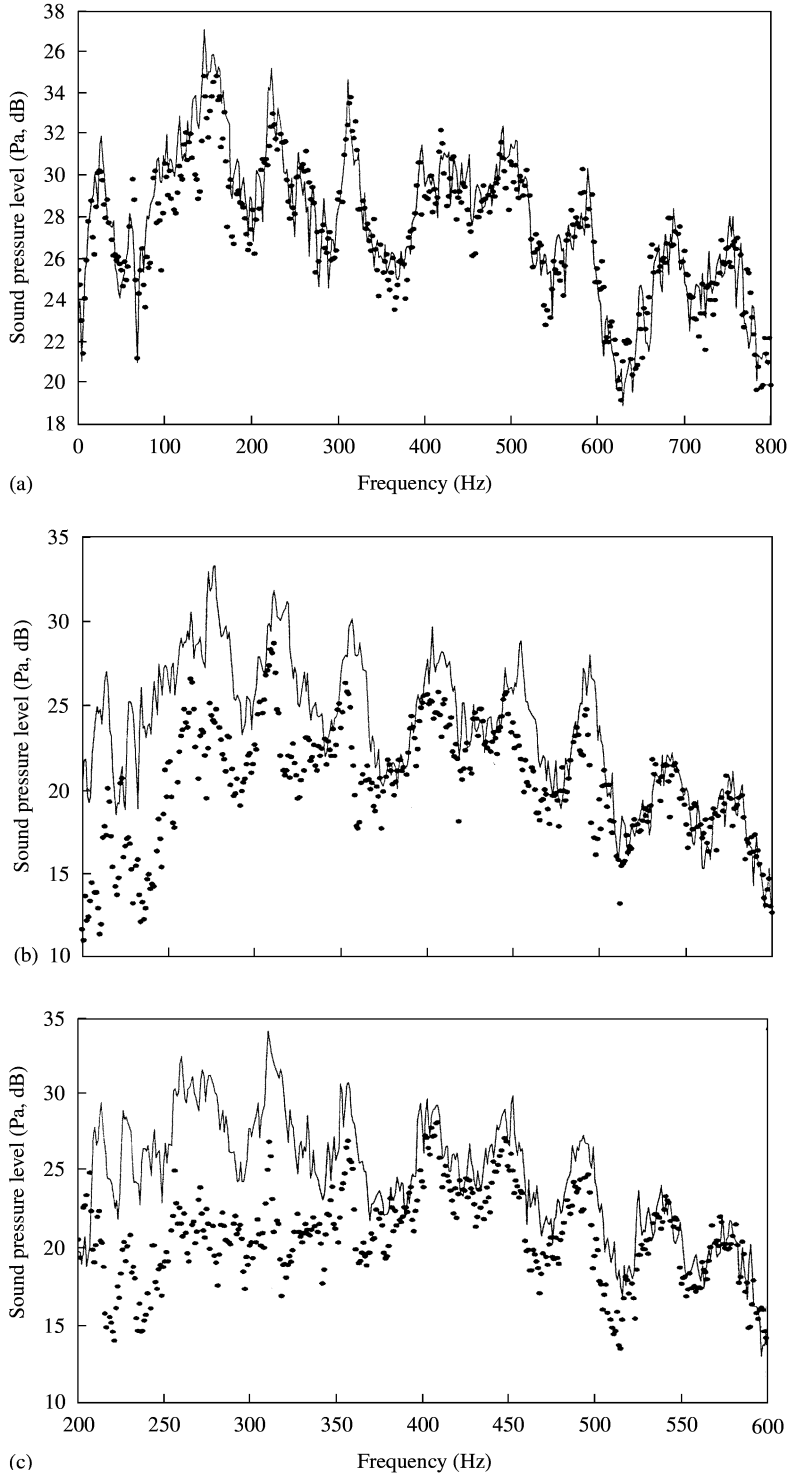

Figure 6. Experimental results of some commonly used LMS-based ANC algorithms. (a) The control performance of FXLMS implementation; (b) the control performance of feedback neutralization implementation; and (c) the control performance of FULMS implementation. ——, Control off; ……, control on.

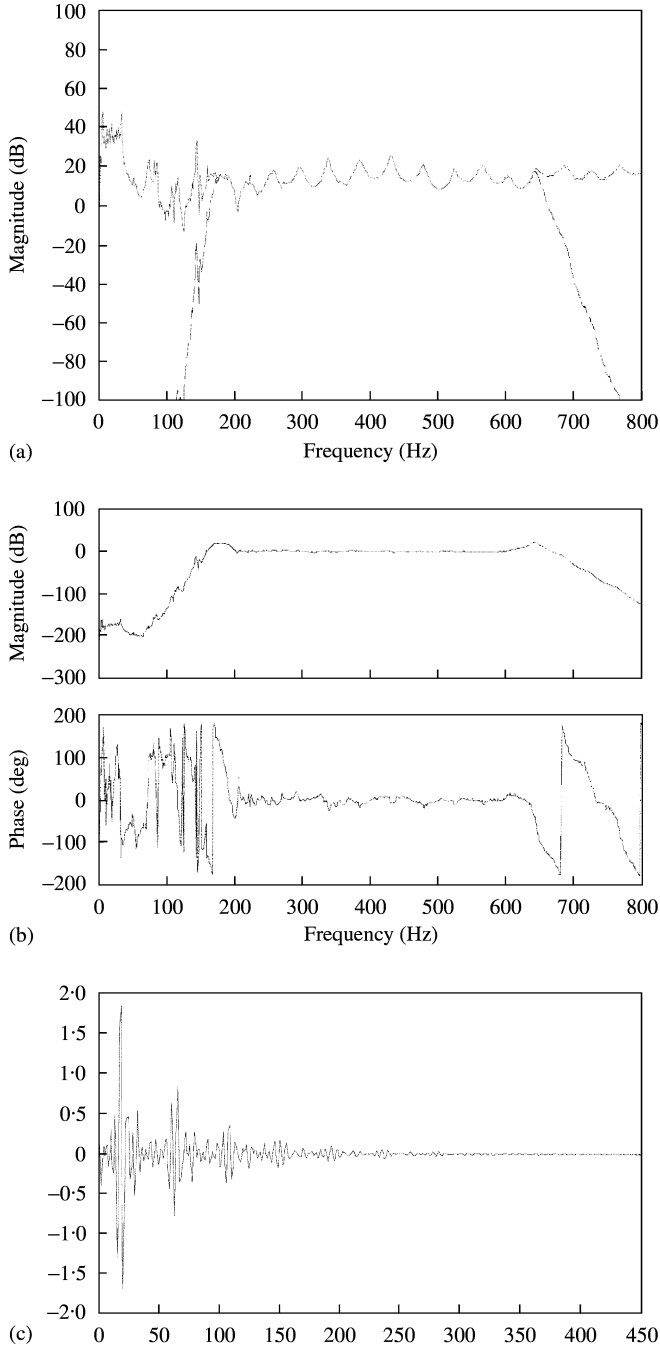

Figure 7. Design of spatially feedforward controller. (a) The frequency response of the IIR filter: ——, Roure's controller; – – – –, second order IIR filters; (b) the frequency response of the FIR filter of the adaptive spatially feedforward controller; and (c) the impulse response of Roure's controller.

invfreqz converts the frequency response of the IIR filter into a transfer function which in turn is converted by using *tf*2*sos* into second order transfer functions for DSP implementation. The result of this procedure is schematically shown in Figure 7(a). Third,

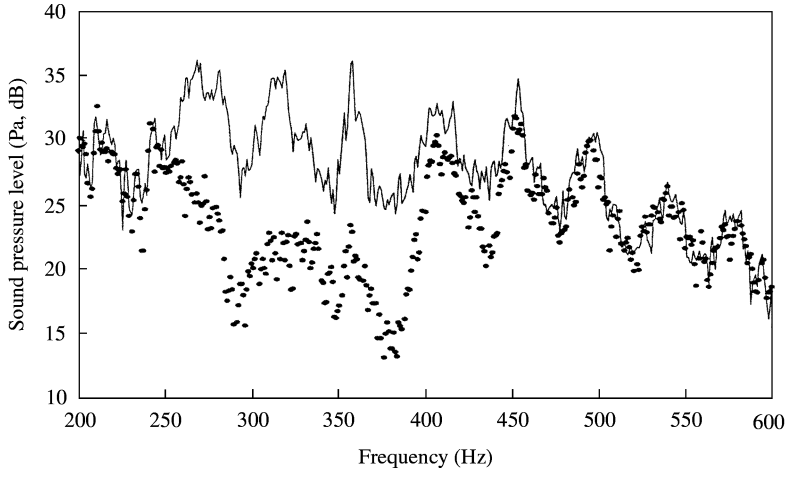

Figure 8. The control performance of the adaptive spatially feedforward algorithm. ——, Control off; ……, control on.

TABLE 1

Comparison of ANC methods

Items	FXLMS algorithm	Feedback neutralization algorithm	FULMS algorithm	Adaptive spatially feedforward algorithm
Control bandwidth (Hz)	200–600	200–600	200–600	200–600
Filter length of secondary path	128	128	128	128
Filter length of feedback path		256		
The feedforward filter length			30	
The feedback filter length			30	
The order of IIR filter				20
Length of adaptive filter	256	256		50
Scaling factor	0·5	0·25	0·5	0·5
Step size	− 1·0	− 0·8	− 0·3	− 0·1
Total band attenuation (dB)	0·4	3·2	3·8	4·2

the FIR part of C is adaptively updated by LMS algorithm with a reference signal that is the output of the IIR filter. In the block diagram of Figure 5, the FIR filter follows the IIR filter and the cascaded filter approximates the ideal controller C in equation (11). As shown in the results of Figures 7(a) and 7(c), the implemented controller exhibits the aforementioned repetitive patterns in the frequency response and in the impulse response as well. Using the adaptive spatially feedforward algorithm, the experimental result of control performance is obtained (Figure 8). The experimental results of the FXLMS algorithm, the feedback neutralization algorithm, the FULMS algorithm, and the adaptive spatially feedforward algorithm are summarized in Table 1. It can be observed in the results that the adaptive spatially feedforward algorithm yields the best performance in the total control bandwidth (4·2 dB). In addition, the adaptive spatially feedforward algorithm requires fewer taps of the

filter than the other methods. Although significant attenuation in total band is obtained using adaptive spatially feedfordward algorithm, the performance in the frequency band near 200 and 500 Hz is not as good. This is due to the fact that the gain in that frequency region is not sufficiently high to produce enough control output.

4.2. SOME IMPLEMENTATION ISSUES

First, the secondary path and feedback path can be reliably modelled off-line via inverse fast Fourier transform and are realized by FIR filters. Sufficient lengths are required to capture the fully decayed impulse responses.

The adaptive spatially feedforward algorithm approximates the physical nature of the transducer dynamics (FIR part) and the repetitive controller of the Munjal's ideal controller (IIR part) respectively. Because the lightly damped dynamics of the repetitive controller has been represented by an IIR filter, only an FIR filter of very low order, e.g., 50 coefficients is needed to represent the remaining dynamics of the controller. The frequency response of the FIR filter can be predicted by dividing Roure's controller by IIR filter. The LMS algorithm should converge to this fixed FIR filter. Figure 7(b) illustrates the frequency response of the FIR filter that is nearly a constant gain.

Another implementation issue is regarding the effect of scaling on the convergence speed. From the following relation [12]:

$$0 < \mu < \frac{1}{p_{x'}(L + \Delta)}, \tag{16}$$

where μ is the step size, L is the length of the adaptive filter, Δ is the delay of the secondary path, and $p_{x'}$ is the power of the filtered reference signal. The speed of convergence can be improved by having a greater step size μ by decreasing $p_{x'}$. This can be done in the DSP program by multiplying the reference signal by a scaling factor, M, to decrease $p_{x'}$ and dividing the control output by the same factor M.

5. CONCLUSIONS

In the paper, an adaptive spatially feedforward algorithm has been developed. The ideal controller derived in section 2 via Roure's approach has proved that it can be partitioned into two parts: an FIR filter and an IIR filter. In the case where the temperature of the duct is not varied much, the repetitive peaks of the ideal controller are almost fixed. Thus, the IIR part representing a repetitive controller is implemented as a fixed controller, whereas the FIR part representing the transducer dynamics is implemented by an adaptive LMS filter to accommodate perturbations and uncertainties in the system.

The proposed technique was compared with commonly used methods such as the FXLMS algorithm, the feedback neutralization algorithm, and the FULMS algorithm by means of extensive experimental investigations. Among these ANC approaches, the proposed technique attains the best performance of noise attenuation (4·2 dB, total band), even in the presence of acoustic feedback.

In our experiments, the plant and the secondary path are modelled off-line. It is reported in Eriksson's work [14] that an adaptive controller with online plant modelling is capable of tracking plant variations. Future research will be focused on this particular aspect.

ACKNOWLEDGMENTS

The present work was supported by the National Science Council in Taiwan, Republic of China, under the project number NSC 87-2212-E009-022.

REFERENCES

1. S. J. ELLIOTT and P. A. NELSON 1993 *IEEE Signal Processing Magazine* **10**, 12–35. Active noise control.
2. P. A. NELSON and S. J. ELLIOT 1992 *Active Control of Sound*. London: Academic Press.
3. M. A. SWINBANKS 1973 *Journal of Sound and Vibration* **27**, 411–436. The active control of sound propagation in long ducts.
4. S. M. KUO and D. R. MORGAN 1995 *Active Noise Control Systems*: *Algorithms and DSP Implementations*. New York: John Wiley and Sons.
5. M. R. BAI and Z. LIN 1998 *American Society of Mechanical Engineers Journal of Vibration Acoustics* **120**, 958–964. Active noise cancellation for a three-dimensional enclosure by using multiple-channel adaptive control and H_∞ control.
6. R. F. LA FONTAINE and I. C. SHEPHERD 1983 *Journal of Sound and Vibration* **91**, 351–362. An experimental study of a broadband active attenuator for cancellation of random noise in ducts.
7. J. HONG and D. S. BERNSTEIN 1998 *IEEE Control Systems Technology* **6**, 111–120. Bode integral constraints, colocation, and spillover in active noise and vibration control.
8. M. L. MUNJAL and L. J. ERIKSSON 1988 *Journal of Acoustical Society of America* **84**, 1086–1093. An analytical, one-dimensional, standing-wave model of a linear active noise control system in a duct.
9. M. T. S. TOMIZUKA and K. K. CHEW 1989 *American Society of Mechanical Engineers Journal of Dynamic Systems, Measurement, and Control* **111**, 353–358. Analysis and synthesis of discrete-time repetitive controllers.
10. A. ROURE 1985 *Journal of Sound and Vibration* **101**, 429–441. Self-adaptive broadband active sound control system.
11. M. R. BAI, J. D. WU and Y. J. LIN 2001 *American Society of Mechanical Engineers Journal of Vibration and Acoustic* **123**, 129–136. Analysis and DSP implementation of a broadband duct ANC system using spatially feedforward structure.
12. S. M. KUO and D. R. MORGAN 1996 *Active Noise Control System*. New York: John Wiley.
13. A. GRACE, A. J. LAUB, J. N. LITTLE and C. M. THOMPSON 1999 *Matlab Control System Toolbox*. Natick, MA: The Math Works, Inc.
14. L. J. ERIKSSON and M. C. ALLIE 1989 *Journal of the Acoustical Society of America* **85**, 797–802. Use of random noise for on-line transducer modeling in an adaptive active attenuation system.